JOURNAL OF MATERIALS SCIENCE 37 (2002) 1593–1597

# Evaluation of hot workability of particle reinforced aluminum matrix composites by using deformation efficiency

DO-HYUN PARK, BYUNG-CHUL KO, YEON-CHUL YOO
*School of Materials Science and Engineering, Inha University, Inchon 402-751, Korea*
*E-mail: ycyoo@inha.ac.kr*

The high temperature deformation behavior of Al 6061 composites reinforced with SiC and $Al_2O_3$ particles has been studied in the temperature range of 300–550°C and the strain rate range of 0.1–3.0/sec by hot torsion test. The deformation efficiency $\eta$, given by $(2m/m+1)$, where $m$ is the strain rate sensitivity, is calculated as a function of temperature and strain rate to obtain iso-efficiency contour map. The composite reinforced with SiC particle exhibited a domain of dynamic recrystallization (DRX) with a peak efficiency of ~40% at the temperature range of 450–500°C and strain rate range of 0.2–0.5/sec. On the other hand, the composite reinforced with $Al_2O_3$ particle showed the DRX domain at the temperature range of 450–480°C and strain rate range of 0.1–0.2/sec. The characteristics of these domain have been investigated with the help of microstructural observation and hot ductility measurements. 

## 1. Introduction

Discontinuously reinforced metal-matrix composites (MMCs) based on Al are recognized as important structural materials because of its superior properties such as high specific strength, high-temperature resistance, and reduced thermal expansion coefficient [1, 2]. Also, these MMCs have the advantage of amenability to secondary metal working processes like extrusion, rolling, and forging compared to continuously reinforced composites [3]. However, the MMCs show a lower hot ductility than the monolithic alloy owing to the presence of reinforcements during hot working. Thus, to improve the hot workability of the Al-based composites, it is necessary to understand the hot deformation behaviors and the effects of deformation conditions on deformed microstructure and hot-ductility during the processing.

The aim of this work is to study the hot working behavior of two types of Al matrix composites containing different ceramic particles and to generate a iso-efficiency contour map for the optimization of hot workability. The map, which is based on dynamic materials model (DMM) [4], shows materials behavior under hot working and was established to reveal the relationship between deformation efficiency and their microstructure. For example, Prasad et al. has suggested the optimum hot working condition for Al-based composites and other materials by using deformation efficiency and its corresponding microstructure [5, 6]. In this model, the workpiece was considered as a dissipator of power and at any instant the total power dissipated consisted of two parts: $G$ content representing the temperature rise and $J$ co-content representing the dissipation through microstructural changes.

The $J$ co-content is given by

$$J = \sigma\dot{\varepsilon}m/(m+1)$$

where $\sigma$ is the flow stress and $\dot{\varepsilon}$ is the strain rate.

For an ideal linear dissipator, $J = J_{max} = \sigma\dot{\varepsilon}/2$. The variation of deformation efficiency parameter, $\eta = J/J_{max}$ with $\varepsilon$, $\dot{\varepsilon}$, and $T$ represents the characteristics of power dissipation of the workpiece occurring through microstructural changes. The major advantage of this model is that it helps to establish the materials behavior under "dynamic" conditions since the efficiency represents the instaneous power dissipation characteristics. In this study the hot workability of the composites is evaluated by correlating deformation efficiency with microstructural changes during hot deformation.

## 2. Experimental procedure

The materials used in this work were 8 $\mu$m size of SiC and $Al_2O_3$ particles and Al 6061 alloy powders. The composites were fabricated by powder metallurgy. For the fabrication of the composites, the Al alloy powers and $SiC_p$ were ball-milled for 72 hours and the resulting mixtures were compacted by hot pressing at 520°C and 120 MPa in vacuum before cooling. The hot-pressed billets with a diameter of 50 mm and length of 50 mm were hot-extruded with an extrusion ratio of 25 : 1 at 430°C. The Al 6061 composite reinforced with $Al_2O_3$ was fabricated by the same process mentioned above. The torsion specimens with a gauge length of 10 mm and a diameter of 7 mm were machined from the extruded composite bars. The torsion test specimens

were heated to 300–550°C using a dual elliptical radiant furnace and then held for 10 min. The torsion tests were conducted in the temperature range of 300–550°C and strain rate range of 0.1–3.0/sec.

The effective stress $\sigma$ and effective strain $\varepsilon$ of the composites were calculated from the torque moment and angular displacement measured from the torsion tests using the von Mises criterion [7].

Deformation efficiency was calculated from the calculated values of strain rate sensitivity and was used to plotting an iso-efficiency contour map. The microstructures of the as-extruded and fracture surface were examined by the scanning electron microscopy (SEM). Transmission electron microscopy (TEM) was also used to examine the microstructures of the hot-deformed composites. The TEM specimens were mechanically ground to ~60 $\mu$m and then jet-polished with a solution of 25% nitric acid and 75% methanol under a condition of 30 V and 60 mA at about −40°C.

## 3. Results and discussion

The flow stress–strain curves for Al 6061 composites reinforced with $Al_2O_3$ and SiC particles are shown in Fig. 1. The flow curves show a greater hardening behavior compared to the monolithic alloy. This is because of high densities of dislocations created by the difference in coefficients of thermal expansion (Δ CTE) between reinforcements and matrix alloy (Table I) [8].

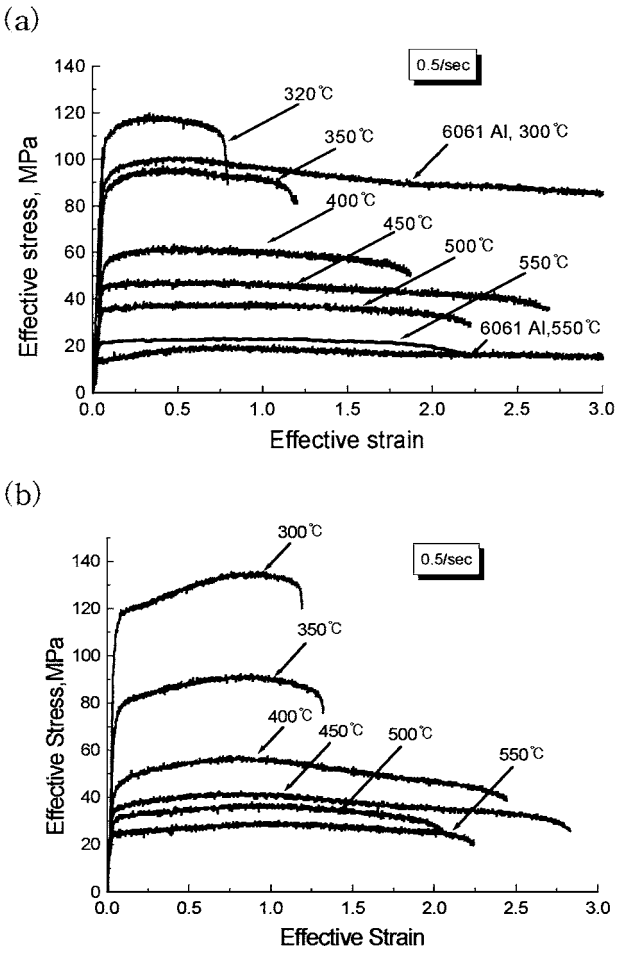


*Figure 1* Effective stress and effective strain curves of Al 6061 composites reinforced with (a) SiC and (b) $Al_2O_3$ particles.

TABLE I The mean coefficient of thermal expansion of aluminum alloy and $Al_2O_3$ and SiC particles

| | CTE($10^{-6}$/°C) | | | | |
|---|---|---|---|---|---|
| | 25–100°C | 25–200°C | 25–300°C | 25–400°C | 25–500°C |
| 6061 | 23.4 | 24.3 | 25.3 | 25.4 | 25.5 |
| $Al_2O_3$ | 6.4 | 6.9 | 7.2 | 7.4 | 7.5 |
| SiC | 3.3 | 3.8 | 4.1 | 4.4 | 4.7 |

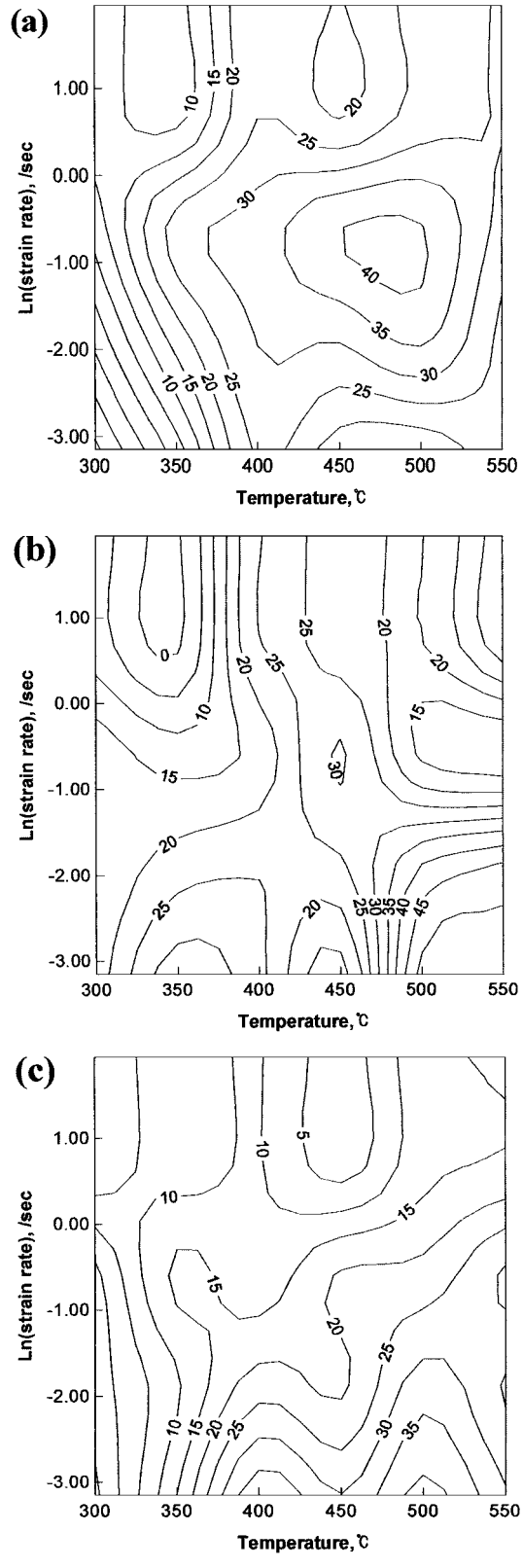


*Figure 2* Iso-efficiency maps of Al 6061 composites reinforced with (a) SiC and (b) $Al_2O_3$ (c) matrix alloy obtained at the strain of 0.4.

The Δ CTE dislocations are created during fabrication, heating and cooling stages. In addition, it has been known that the hardening behavior of the composites strongly depends upon strain rate and temperature. As the temperature rising, the increase of flow stress caused by particle strengthening diminished to smaller values as that of the monolithic alloy [9]. The strengthening of the composites is due to the geometrical constraint of hard rigid particle during plastic flow as well as the increased dislocation density. The reinforcements used in this experiment are angular $Al_2O_3$ and SiC particles, so the difference in flow stress between the composites has been obtained at the efficiency value of 42% (Fig. 2). Also, the hot deformed microstructure at 480°C and 0.1/sec of $Al_2O_3$/Al 6061 composite is shown in Fig. 3b. It is also found that equiaxed dynamic recrystallized grains were obtained in the composite during hot deformation.

The instability map, which is developed by Kumar and Prasad [13], is used for evaluating the regimes of microstructural instabilities for the composites. The metallurgical instability will occur when $dD/d\dot{\varepsilon} < D/\dot{\varepsilon}\,.\,D$, which is related to microstructural changes, is equivalent to $J$ co-content ($J = \sigma\dot{\varepsilon}\,m/(m+1)$), so

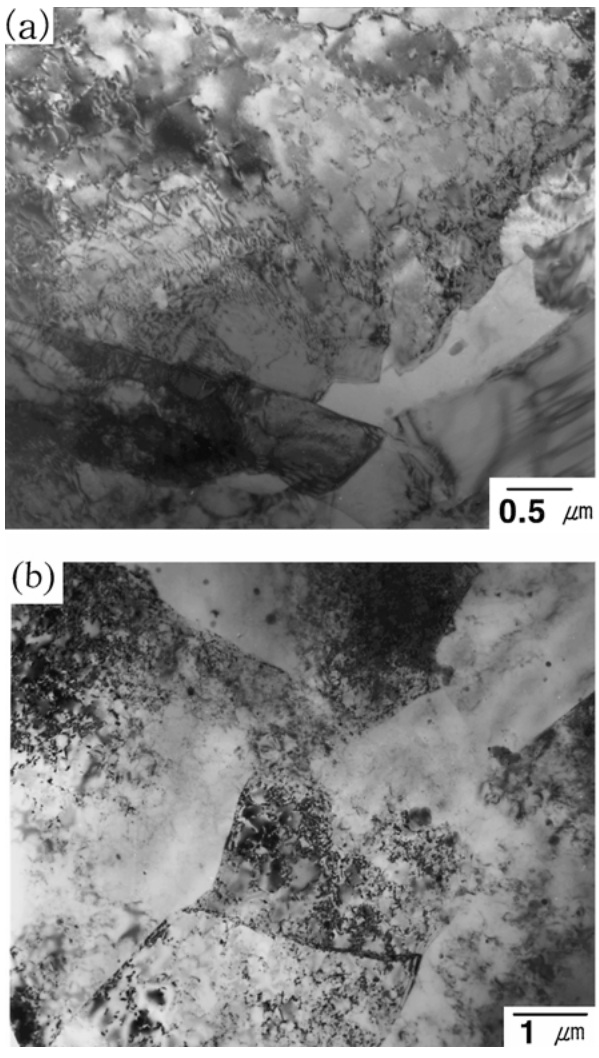


*Figure 3* TEM bright field images of (a) $SiC_p$/Al 6061 composite deformed at 480°C, 0.5/sec and (b) $Al_2O_3$/Al 6061 composite deformed at 480°C and 0.2/sec.

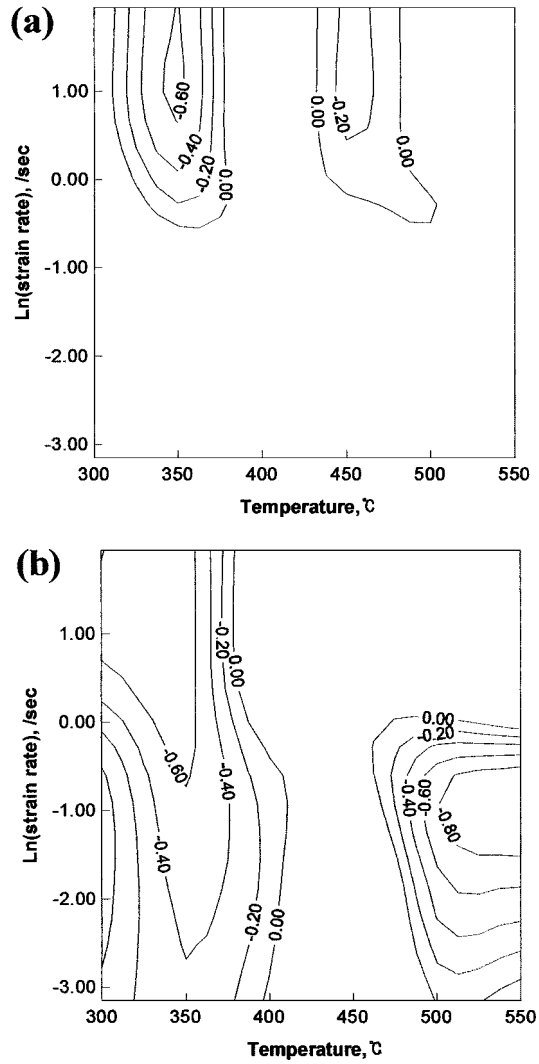


*Figure 4* Instability maps of (a) SiC and (b) $Al_2O_3$ particles reinforced Al 6061 composites and (c) matrix alloy obtained at the strain of 0.4.

the upper equation becomes

$$\frac{\partial \ln(m/m+1)}{\partial \ln \varepsilon} + m < 0$$

The left hand side of this equation is represented by $\xi(\dot{\varepsilon})$, which negative, indicates microstructural instability in the material. The variation of instability parameter $\xi(\dot{\varepsilon})$ with temperature and strain rate is shown in Fig. 4 obtained at the strain of 0.4. The instability regime of $Al_2O_3$/Al 6061 composite is wider than that of $SiC_p$/Al 6061 composite. This is due to the difference of the extent of bonding between matrix and reinforcements. The SiC has well-bonded properties compared to $Al_2O_3$ [13]. Therefore, it would be expected that fewer voids would be attached to SiC particles during deformation. In Fig. 5a, the round shaped voids were easily formed at the matrix/$Al_2O_3$ interface than SiC, indicating that interfacial debonding which lead to local cracking in the end. In Fig. 5b, as a result of observation by SEM, the manifestation of microstructural instability could be known from the formation of cracking due to flow localization. Therefore, the regime of microstructural instability should be avoided to obtain the composites with sound microstructure during hot deformation.

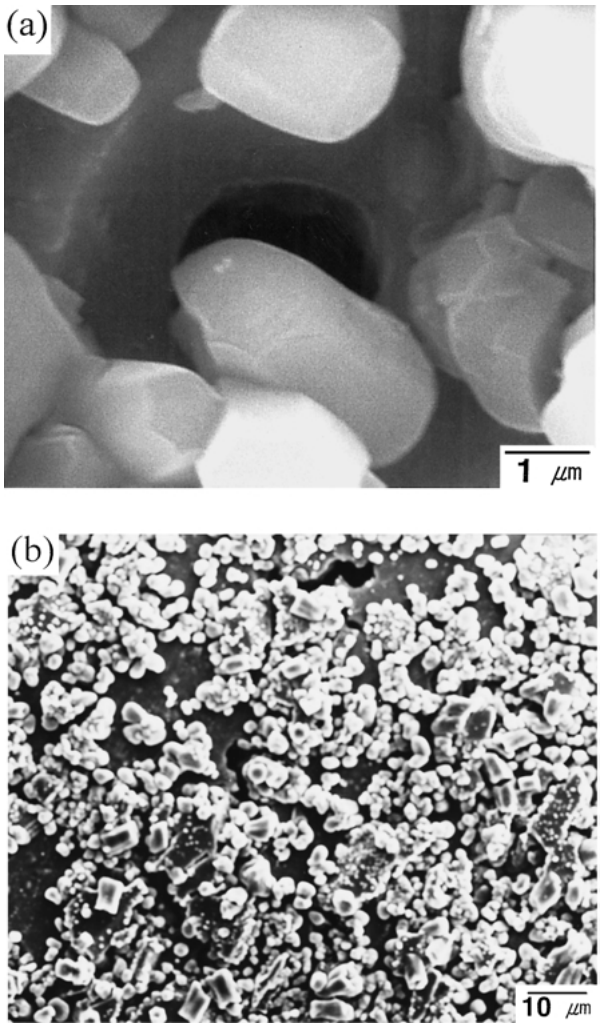


*Figure 5* SEM micrographs of $Al_2O_3$/Al 6061 composite deformed at 550°C and 0.1/sec.

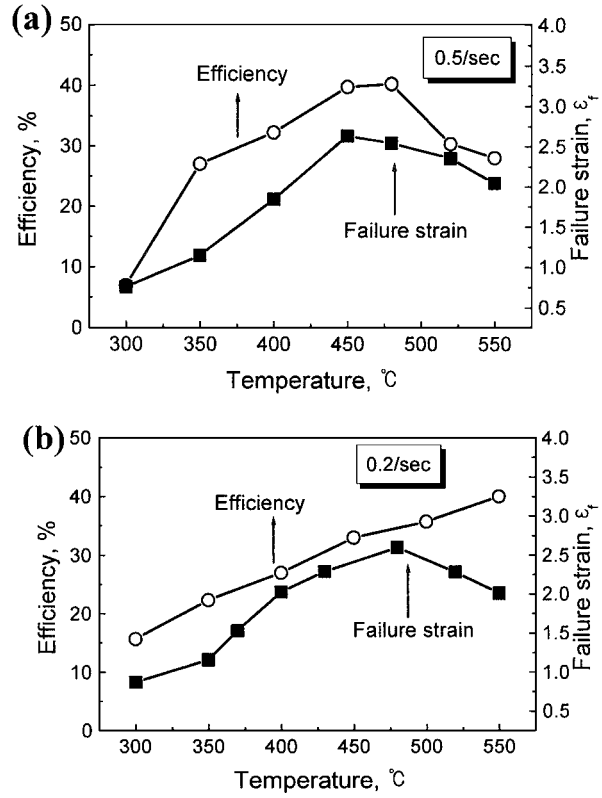


*Figure 6* Variations of failure strain and deformation efficiency with temperature for (a) SiC and (b) $Al_2O_3$ particle reinforced Al 6061 composites.

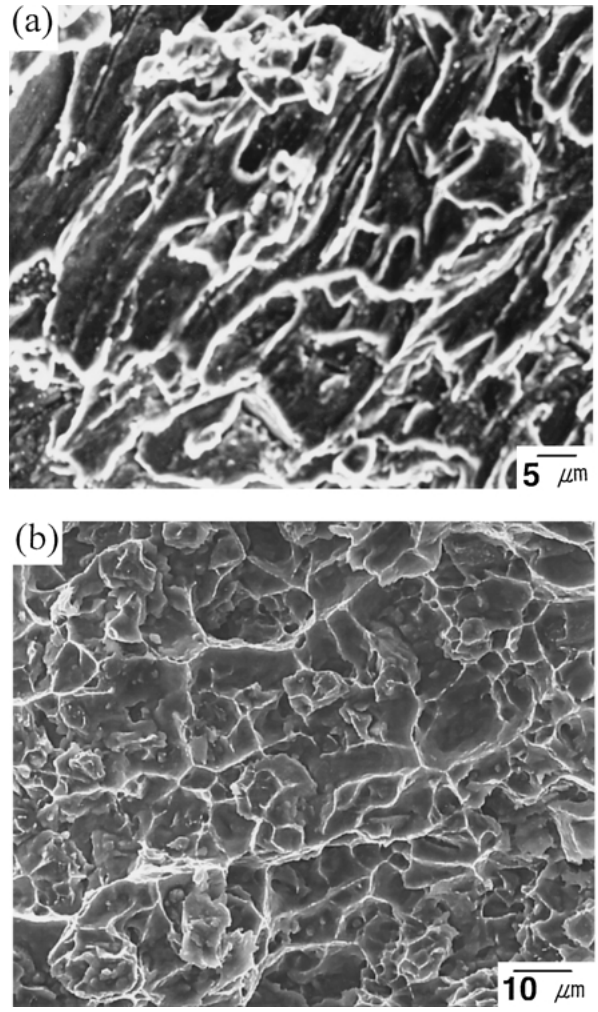


*Figure 7* Fracture surface image (SEM) of (a) $SiC_p$/Al 6061 composite deformed at 480°C, 0.5/sec and (b) $Al_2O_3$/Al 6061 composite deformed at 450°C and 0.2/sec.

The variation of failure strain and deformation efficiency for both composites with strain rate and temperature is shown in Fig. 6. In both cases, the regimes of high failure strain are nearly coincided with the DRX occurrence. The microstructure of fracture surface for Al6061 composite reinforced with (a) SiC and (b) $Al_2O_3$ obtained at 480°C, 0.5/sec and 450°C, 0.2/sec respectively are shown in Fig. 7. It showed ductile-fractured surface with prolonged formed dimples along the deformation direction. The variation of failure strain with temperature and strain rate showing DRX behavior similar to that of the deformation efficiency. But in Fig. 6b, the deformation efficiency obtained at high temperature (>500°C) is higher than that of obtained at DRX domain. It has been reported that the damage process such as void formation, wedge cracking and grain boundary cracking are very efficient in dissipating power as well as superplasticity and they were characterized by a steep rise in efficiency with decrease of strain rate [15]. In order to confirm the superplasticity, it is important to measure failure strain of the composites. Normally, large strains are obtained during superplastic deformation. In this experiment, the composites exhibited small strains less than 260% resulting from the generation of voids due to flow localisation. Therefore, to obtain DRX microstructure and good ductility of the

composites, the deformation efficiency should be considered including the microstructural changes under the considered deformation conditions.

## 4. Conclusions

The hot deformation behavior of Al 6061 composites reinforced with 15v.%SiC and $Al_2O_3$ particles is studied in the temperature range 300–550°C and strain rate range 0.1–3.0/sec by using deformation efficiency and the following conclusions are drawn from the results.

1. There is no significant effect of strain on iso-efficiency map for the composites unlike temperature and strain rate.

2. The $SiC_p$/Al 6061 composite showed an efficiency of ∼40% at the DRX domain of 450–500°C and 0.2–0.5/sec, while for the $Al_2O_3$/Al 6061 composite, DRX domain occurs at 450–480°C and 0.1–0.2/sec showing an efficiency of ∼35%.

3. The instability regimes of $Al_2O_3$/Al 6061 composite are wider than those of $SiC_p$/Al 6061 composite because of difference in strength of reinforcements.

4. The variation of failure strain as a function of temperature and strain rate is similar to that of the deformation efficiency.

## References


1. C. G. E. MANGIN, J. A. ISAACS and J. P. CLARK, *JOM* **48** (1996) 49.
2. G. CURRAN, *The J. of the Inst. Mater. World* **6** (1998) 20.
3. P. DIVECHA, S. G. FISHMAN and S. D. KARMARKAR, *J. Met.* **33** (1981) 15.
4. E. S. PUCHI and M. H. STAIA, *Metall. Trans.* A **26** (1995) 2895.
5. Y. V. R. K. PRASAD, H. L. GEGEL, S. M. DORAIVELU, J. C. MALAS, J. T. MORGAN, K. A. LARK and D. R. BARKER, *ibid.* **15** (1984) 1887.
6. B. V. RADHARKRISHNA BHAT, Y. R. MAHAJAN, H. MD. ROSHAN and Y. V. R. K. PRASAD, *Mater. Sci. and Technol.* **15** (1995) 16.
7. K. MILLS, J. R. DAVIS, D. A. DIETERICH, G. M. CRANKOVIC, H. J. FRISSEL, D. M. JENKINS, W. H. CUBBERLY and R. L. STEDFELD, in "Metals Handbook," 9th ed., Vol 8 (American Society for Metals, Metals Park, OH) p. 154.
8. X. XIA, P. SAKARIS and H. J. MCQUEEN, *Met. Soc. CIMM* (1994) 129.
9. B. C. KO and Y. C. YOO, *Mater. Sci. and Technol.* **14** (1998) 766.
10. S. ELOMARI, R. BOUKHILI and D. J. LLOYD, *Acta Met.* **44** (1996) 1878.
11. B. DERBY and M. F. ASHBY, *Scripta Mater.* **21** (1987) 882.
12. B. V. RADHAKRISHNA BHAT, Y. R. MAHAJAN, H. MD. ROSHAN and Y. V. R. K. PRASAD, *Metall. Trans.* A **23** (1992) 2229.
13. Y. V. R. K. PRASAD, *Indian Journal of Technology* **28** (1990) 445.
14. R. L. DEUIS, J. M. YELLUP and C. SUBRAMANIAN, *Mater. Sci. and Technol.* **13** (1997) 521.
15. S. VENUGOPAL, S. L. MANNAN and Y. V. R. K. PRASAD, *Metall. Trans.* A **22** (1991) 829.



*Received 21 March*
*and accepted 11 December 2001*